Speed Improvement of a Non-Contact Mode Atomic Force Microscopy (AFM) using Hybrid MPC-PI Control

Muhammad Umair, Prof. Kyihwan Park*

Abstract— **Atomic Force Microscopy (AFM) has revolutionized nanoscale characterization by offering high-resolution imaging for a wide range of surfaces. Among its operating modes, the non-contact mode AFM (NC-AFM) is particularly valuable for preserving the integrity of soft and biological structures by minimizing intrusive forces between the sample and the cantilever tip. However, conventional NC-AFM suffers from slow scanning speeds, making it unsuitable for capturing real-time dynamic processes that require high data acquisition rates. This limitation primarily arises from transient behavior due to the cantilever's mass and the delay introduced by the root-mean-square (RMS) circuit traditionally used for demodulating the oscillating sensor signal.**

To enhance imaging speed, this paper presents a hybrid control strategy combining Model Predictive Control (MPC) and Proportional-Integral (PI) control. In this approach, MPC moves the cantilever closer to the sample in open-loop operation, thereby reducing the gap distance for the PI feedback control. This hybrid method allows the piezoelectric (PZT) actuator to follow the sample surface more accurately and at higher speeds, achieving up to 10 scan lines per second (10 Hz)—five times faster than conventional method. Experimental validation using a 100nm step-shaped sample demonstrates the enhanced performance of the proposed controller.

I. Introduction

Atomic Force Microscopy (AFM) is widely recognized for its ability to perform three-dimensional, high-resolution imaging at the atomic scale. Unlike other microscopy techniques, AFM operates without strict constraints on sample material or environmental conditions, making it highly versatile for surface characterization. AFM primarily operates in two fundamental modes: contact mode (CM-AFM) and non-contact mode (NC-AFM) [1].

In CM-AFM, the cantilever tip remains in continuous contact with the sample surface during scanning, allowing direct measurement of surface topography. The deflection of the cantilever is directly measured by the photodiode (PD) sensor, enabling faster scanning in CM-AFM compared to NC-AFM. This mode offers higher spatial resolution and faster feedback, making it suitable for imaging hard surfaces with fine details. It also allows for direct force interaction with the sample, which is essential for precise topographical and mechanical property measurements.

In NC-AFM, the cantilever oscillates near its resonance frequency and hovers above the sample surface without making physical contact. Its oscillation amplitude is modulated by attractive forces between the tip and the sample [2]. Since its invention [3, 4], NC-AFM has been increasingly used to image a wide range of samples due to its ability to minimize tip wear and sample damage, making it ideal for delicate structures. However, the slow imaging speed of NC-AFM remains a significant limitation, particularly when analyzing dynamic biological processes occurring on the microsecond scale.

The primary factors limiting NC-AFM's speed are the mass of the cantilever and the time delay introduced by the demodulation process required to extract topographical information [5]. When the cantilever moves between different surface heights, its inherent mass causes the oscillation amplitude to vary with the gap, leading to a transient response before a steady-state amplitude is reached. Additionally, the root-means-square (RMS) circuit which is used for demodulation of sensing signal into a DC value to extract the gap distance, introduces further time delays. These factors collectively slow down the scanning process and limit the imaging speed. Furthermore, non-linear characteristics of NC-AFM also results in varying settling times for different gap distances.

To address these challenges, researchers have explored both hardware-based and control-based approaches. Hardware solutions [6-11], such as miniaturizing cantilevers and actuators, can increase system bandwidth but often come at the cost of reduced scan range. In contrast, control-based methods [12-16], including Q-control, feedforward compensation, dynamic PID control, and repetitive control, offer improvements in speed with minimal additional cost. However, these techniques either achieve only modest increases in imaging speed or trade off image quality and sample preservation.

Muhammad Umair received his MS in Mechanical Engineering from School of Mechanical and Robotics Engineering, Gwangju Institute of Science and Technology (GIST), South Korea. He is currently working as Mechanical Design Engineer in WeGo-Robotics South Korea.

Prof. Kyihwan Park is with the School of Mechanical and Robotics Engineering, Gwangju Institute of Science and Technology (GIST), South Korea.

(*Corresponding Author: khpark@.gist.ac.kr).

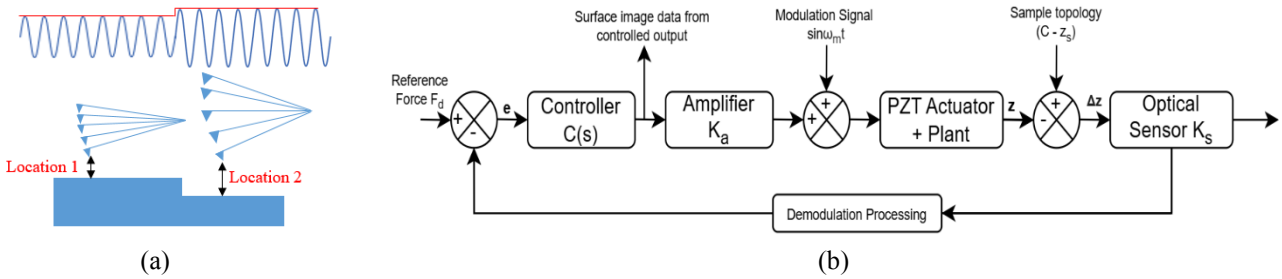

Figure 1. AFM non-contact mode imaging: (a) schematic diagram, (b) block diagram of conventional PI feedback approach. C(s), Ka, Ks, represent the controller, gain of PZT amplifier, and sensor gains.

A conventional PI controller is commonly used for gap control in AFM imaging, but its control action is purely reactive. It applies full effort to reach the target without considering the optimal trajectory for the cantilever's movement. Model Predictive Control (MPC) has gained significant popularity in industry due to its ability to handle complex systems, constraints, and optimize control actions based on a known plant model. MPC as a real-time control approach has been successfully applied in CM-AFM imaging to enhance performance [17,18].

In this paper, we propose a hybrid MPC-PI control framework for NC-AFM imaging. In the proposed approach, an MPC is integrated in the feedforward path to compute optimal control inputs to the PZT actuator. It moves the PZT actuator close to the sample based on a state-space model of AFM dynamics, while a proportional-integral (PI) controller takes over at very short gap distances to maintain precise tip-sample interaction. The MPC utilizes real-time sensing signals and topography-related errors from previous scanlines to predict actuator behavior and reduce transient effects, enabling faster tip positioning. By incorporating a disturbance prediction scheme based on sample topography, this approach anticipates surface variations and adjusts the control effort accordingly. The remaining small errors, arising from modeling uncertainties and nonlinear effects such as hysteresis and creep in the piezoelectric (PZT) actuator, are compensated by the PI controller. Experimental results demonstrate that the proposed hybrid MPC-PI control framework significantly enhances imaging speed—achieving more than a fivefold improvement over conventional NC-AFM methods—while maintaining high imaging quality and minimizing tip-sample interaction forces.

II. NON-CONTACT MODE AFM

A. *Topology Construction*

Figure 1 shows the NC-AFM configuration. The cantilever oscillates near its resonance frequency, and as the tip approaches the sample surface, attractive forces reduce the oscillation amplitude. This amplitude is monitored using a photodiode (PD) sensor and converted into a DC value using a demodulation processing circuit such as Root-Mean-Square (RMS) circuit. The DC value is compared with a predefined feedback set point (reference force f_d) to calculate the difference. To minimize it (error), a PI controller (Cs) adjusts its output signal, and then this control output is amplified using an amplifier with gain Ka. The amplified signal controls the Z-scanner displacement in the vertical direction to recover the cantilever amplitude back to its initial set point value. Through the feedback process, the error approaches zero, ensuring accurate surface measurements. Under the assumptions there are no dynamics in the amplifier and PZT actuator with zero steady-state error, the controller output is considered as the sample topography.

B. *Limitation of non-contact mode AFM*

In a CM-AFM, the cantilever is in continuous contact with the sample surface during scanning, the sensing signal that is proportional to the deflection of the cantilever is directly obtained using a PD sensor [19] with a reasonably high speed. However, in NC-AFM, we need to consider the mass effect of the cantilever which floats on the air without contact. Figure 2 shows the signal measured when the cantilever moves from one point on the sample to a higher location. It is shown that the amplitude of oscillations increases as the gap increases. A transient response due to the mass effect of the cantilever is also observed before the signal reaches a steady state when the location change occurs. This transient response significantly contributes to the slow scanning speed of NC-AFM. Additionally, we need demodulation processing, i.e. RMS circuit to convert the sensing signal to a DC-value corresponding to the gap distance between a sample and cantilever. The algorithm of mean in the RMS circuit causes the time delay as shown in the dotted line in Figure 2.

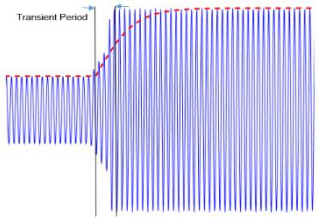

Figure 2 A sensing signal measured when the cantilever moves from one point on the sample to a higher location

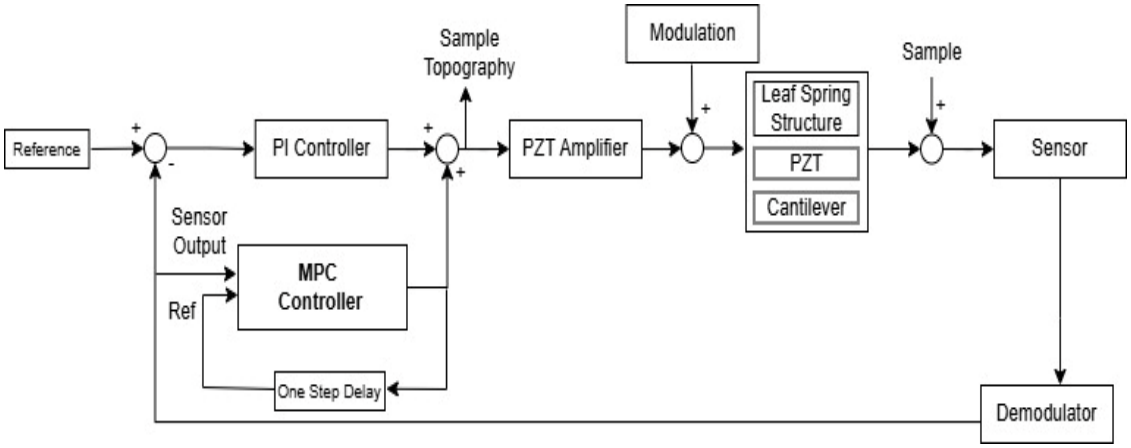

Figure 3 Block diagram of proposed hybrid MPC-PI Controller.

In conclusion, it can be said that the mass of cantilever and demodulation processing time of a sensor are main reasons for the slow speed of NC-AFM

Since it is inevitable to use a cantilever, the slow speed of the NC- AFM is ultimately affected by a sensor that needs to be used for closed loop control. Therefore, a strategy to reduce sensing time, and the gap distance can help speed up NC-AFM scanning. It can be achieved by moving the PZT actuator close to the sample using open-loop control based on system model and only controlling the PZT actuator at a very short gap distance from the sample using closed-loop control.

C. Advantages of Proposed Method

Conventionally, a PI controller was used with a sensor for entire gap distance control between the cantilever and sample surface to compensate for the errors occurred by parameter uncertainties of the mechanical components and the nonlinearities of the PZT actuator in NC-AFM. The nonlinear characteristics of the NC-AFM result in varying settling times for different distances. Thus, a larger gap distance leads to a longer settling time in the closed loop control. Therefore, by using the above strategy to move the PZT actuator close to the sample using open loop control and only controlling the PZT actuator at a very short gap distance using closed loop control, the settling time has been greatly reduced compared to the conventional PI controller.

III. HYBRID MODEL PREDICTIVE CONTROL (MPC) AND PI IMAGING

To address the slow scanning speed of NC-AFM, MPC is integrated into the PI feedback path as shown in Figure 3. The control action of MPC is achieved based on a known model of the plant; Therefore, the controlled output signal of MPC sends a command to approach the tip to a near-target position and keep it near the set-point position using model-based prediction, thereby reducing reliance on slow feedback dynamics that typically limit NC-AFM performance. The remaining small error resulting from modeling uncertainties, hysteresis and creep effects of the PZT actuator is compensated by using the PI controller in the feedback loop. Additionally, introducing MPC in the loop enhances the overall system gain, providing the benefit of reducing the controller's settling time.

A. Modeling of Non-Contact Mode AFM

The performance of MPC depends upon the mathematical model of the plant. It is difficult to derive the mathematical model of AFM analytically due to complexities lying in the PZT actuator and nonlinearities present at tip-sample interaction. Due to this modeling of AFM is typically achieved through experimental system identification technique [20]. Figure 4 shows the experimental configuration of NC-AFM to obtain the open-loop response, the measured open-loop response is shown in Figure 5.

Then measured open-loop response was processed in MATLAB, and a 4th-order discrete state-space model of the plant was estimated, matching 85% of the measured open-loop response.

$$A_d = \begin{bmatrix} 0.08845 & -0.9311 & -0.3272 & -0.4141 \\ 0.5913 & 0.4476 & -0.1761 & -0.2696 \\ 0.385 & 0.8251 & 0.9391 & -0.1016 \\ 0.07251 & 0.2365 & 0.5051 & 0.9863 \end{bmatrix} \quad (1)$$

$$B_d = \begin{bmatrix} 0.01848 \\ 0.01203 \\ 0.004532 \\ 0.0006122 \end{bmatrix} \quad (2)$$

$$C_d = [670.3 \quad -152 \quad 60.43 \quad -555.4] \quad (3)$$

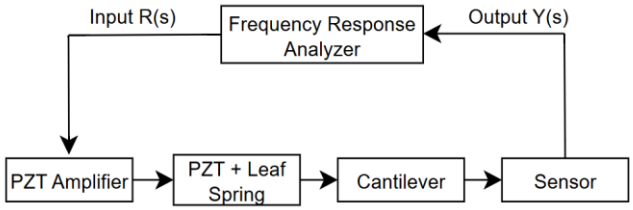

Figure 4. Experimental Setup for measuring open loop response of NC-AFM.

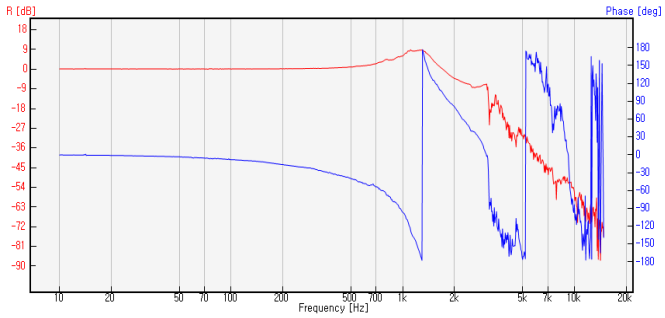

Figure 5. Measured open loop response of NC-AFM.

B. Design of Model Predictive Control

An MPC controller without integral action [21] is used in this research, as an example. The basic architecture of MPC, as illustrated in Figure 6, relies on the principle of predictive optimization over a finite time horizon. At each sampling instant, the controller utilizes a discrete-time model of the system to forecast future outputs based on historical and current input-output data, as well as a sequence of anticipated control actions. These predicted outputs are compared against a predefined reference trajectory, and the resulting error signals are used to formulate a constrained optimization problem. The optimizer solves this problem by minimizing a quadratic cost function that typically balances output tracking accuracy with control effort, while adhering to operational constraints such as actuator saturation or rate limits. Only the first element of the optimized control sequence is applied to the system, after which the horizon shifts forward in time and the procedure is repeated in the next cycle, enabling closed-loop performance with predictive foresight.

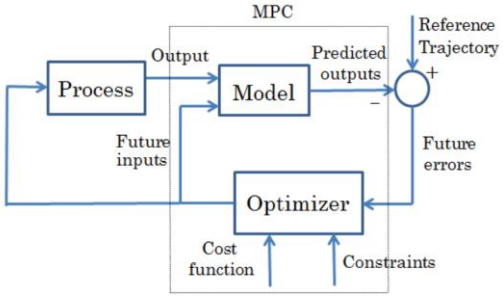

Figure 6. Structure of Model Predictive Control.

The linear system model, which includes a piezo amplifier, z-piezo actuator, cantilever, and sensor dynamics can be described by the following discrete state equations:

$$X(k+1) = Ax(k) + Bu(k) \quad (4)$$

$$y(k) = Cx(k) \quad (5)$$

Matrices A, B, and C represent the plant model. When the system current state vector *x(k)* and control signal *u(k)* are known, we can predict the output Y for the future prediction horizon (*Np*) and control horizon (*Nc*) as:

$$Y = Fx(k_i) + H\Delta U \quad (6)$$

With

$$Y = \begin{bmatrix} y(k+1) \\ y(k+2) \\ \cdot \\ \cdot \\ \cdot \\ y(k+N_p) \end{bmatrix}_{N_P x 1},$$

$$F = \begin{bmatrix} CA \\ CA^2 \\ \cdot \\ \cdot \\ \cdot \\ CA^{Np} \end{bmatrix}_{N_P x 1}$$

$$U = \begin{bmatrix} u(k+1) \\ u(k+2) \\ \cdot \\ \cdot \\ \cdot \\ u(k+Nc) \end{bmatrix}_{N_c x 1}$$

$$H = \begin{bmatrix} CB & 0 & 0 & \dots & 0 \\ CAB & CB & 0 & \dots & 0 \\ CA^2B & CAB & CB & \cdots & 0 \\ \vdots & \vdots & \vdots & \vdots & \vdots \\ CA^{N_p-1}B & CA^{N_p-2}B & CA^{N_p-3}B & \cdots & CA^{N_p-N_c}B \end{bmatrix}$$

The MPC tries to minimize the following objective function at each time step:

$$J = (R-Y)^T Q(R-Y) + U^T W U \quad (7)$$

where *R* represents the reference trajectory over *Np* and *Y* denotes the predicted systems outputs. The objective function in MPC strives to achieve two main goals: first, to follow a reference trajectory by minimizing the error, and second, to

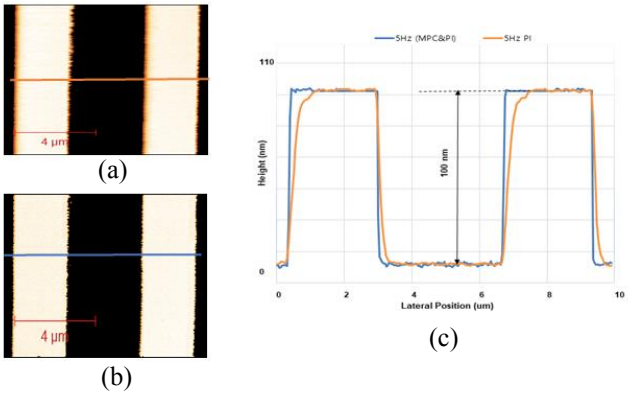

Figure 7. Sample topography of 100nm sample obtained using NC-AFM scanning technique: (a) using the conventional method at 5 scan lines/s (5Hz), (b) using the proposed hybrid method at 5Hz, and (c) the corresponding topography of these scans.

reduce control effort by penalizing significant variations in the control signal to prevent excessive wear on the actuators and limit energy consumption. The matrices Q and W are positive definite weighting matrices used for the output error and control effort, respectively. A higher Q value places greater importance on accurate tracking, resulting in more aggressive control actions. In contrast, a higher W value penalizes larger control efforts, leading to smoother control signals and less stress on the actuators. While this can improve efficiency and reduce wear, it might come at the cost of slightly less precise tracking, especially for highly dynamic reference signal.

IV. Experimental Result

The performance of the proposed hybrid MPC-PI controller for NC-AFM was compared to the conventional PI approach in terms of improved resolution and speed. The conventional method refers to the standard PI-based closed-loop control used in typical NC-AFM imaging systems. Figure 7 illustrates the scanning images obtained at 5 scan lines per second (5 Hz) using a) conventional method and b) proposed method. Notably, the proposed method accurately captures the step shape of the sample. In contrast, the conventional PI-based method failed to maintain sharp corner details at the same speed. This demonstrates that the proposed method offers improved resolution at the same scanning speed. To further evaluate the performance of the proposed method Figure 8 shows the experimental results when the speed is increased to 10 Hz. To provide a clearer comparison at 10 Hz, first the sample was scanned at 2 Hz and 10 Hz speed with conventional method as shown in Figure 8 a) & b), however in Figure 8 b) the image quality of the conventional method degraded significantly as the speed increased to 10Hz, when same point on the sample was scanned with proposed MPC-PI controller at the speed of 10 Hz the hybrid controller maintained the same high level of quality even at 10 Hz speed. These results at 2Hz and 10Hz highlight the advantage of our approach in delivering both higher quality and higher speed performance.

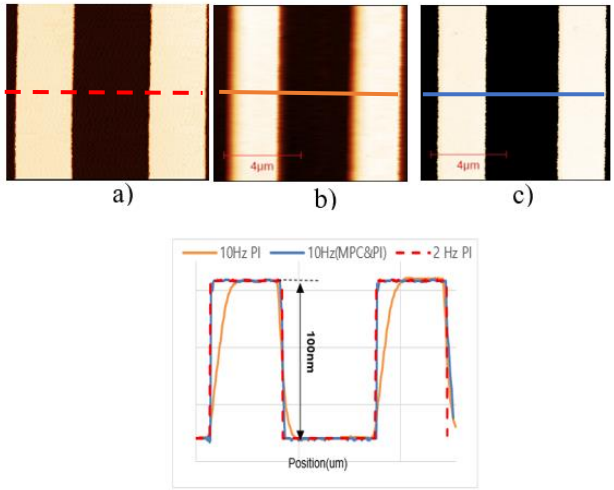

Figure 8. Sample topography of 100nm sample obtained using NC-AFM scanning technique: (a) using the conventional method at 2 Hz, (b) using the conventional method at 10 Hz, (c) using the proposed hybrid method at 10 Hz, and (d) the corresponding topography of these scans.

V. Conclusion

This paper introduces a hybrid MPC-PI control strategy to overcome the slow imaging speed of conventional Non-Contact Mode AFM (NC-AFM). By integrating Model-Predictive Control (MPC) with Proportional-Integral (PI) feedback, the approach minimizes transient delays caused by cantilever dynamics and demodulation process (RMS) circuit. The MPC optimizes open loop positioning to reduce the initial gap distance, while the PI compensates for nonlinearities and uncertainties, enabling precise vertical tracking. Experimental validation on a 100nm step-shaped sample demonstrates a fivefold speed improvement (10 Hz) compared to traditional NC-AFM, while preserving imaging resolution. This advancement enhances NC-AFM's capability for real-time, high-speed nanoscale imaging of dynamic processes in soft and biological samples. While the proposed hybrid MPC-PI control framework demonstrates significant improvements in imaging speed and resolution, several directions remain open for future research. One promising direction is the integration of adaptive or learning-based control schemes, such as reinforcement learning or iterative learning control, to further enhance performance under varying samples topographies or environmental conditions.

VI. References

[1] Abramovitch, D. Y., Andersson, S. B., Pao, L. Y., & Schitter, G. (2007, July). A tutorial on the mechanisms, dynamics, and control of atomic force microscopes. In *2007 American Control Conference* (pp. 3488-3502). IEEE.

[2] Jalili, N., & Laxminarayana, K. (2004). A review of atomic force microscopy imaging systems: application to molecular metrology and biological sciences. *Mechatronics*, *14*(8), 907-945.

[3] Albrecht, T. R., Grütter, P., Horne, D., & Rugar, D. (1991). Frequency modulation detection using high-Q cantilevers for enhanced force microscope sensitivity. *Journal of applied physics*, *69*(2), 668-673.

[4] Martin, Y., Williams, C. C., & Wickramasinghe, H. K. (1987). Atomic force microscope–force mapping and profiling on a sub 100-Å scale. *Journal of applied Physics*, *61*(10), 4723-4729.

[5] Sulchek, T., Yaralioglu, G. G., Quate, C. F., & Minne, S. C. (2002). Characterization and optimization of scan speed for tapping-mode atomic force microscopy. *Review of Scientific Instruments*, *73*(8), 2928-2936.

[6] Balantekin, M. (2015). High-speed dynamic atomic force microscopy by using a Q-controlled cantilever eigenmode as an actuator. *Ultramicroscopy*, *149*, 45-50.

[7] Sahoo, D. R., Sebastian, A., & Salapaka, M. V. (2003). Transient-signal-based sample-detection in atomic force microscopy. *Applied Physics Letters*, *83*(26), 5521-5523.

[8] Sahoo, D. R., Sebastian, A., & Salapaka, M. V. (2004, November). An ultra-fast scheme for sample-detection in dynamic-mode atomic force microscopy. In *2004 NSTI Nanotechnology Conference and Trade Show* (Vol. 3, pp. 11-14).

[9] Schäffer, T. E., Cleveland, J. P., Ohnesorge, F., Walters, D. A., & Hansma, P. K. (1996). Studies of vibrating atomic force microscope cantilevers in liquid. *Journal of applied physics*, *80*(7), 3622-3627.

[10] Ando, T., Kodera, N., Takai, E., Maruyama, D., Saito, K., & Toda, A. (2001). A high-speed atomic force microscope for studying biological macromolecules. *Proceedings of the National Academy of Sciences*, *98*(22), 12468-12472.

[11] Kokavecz, J., Tóth, Z., Horváth, Z. L., Heszler, P., & Mechler, Á. (2006). Novel amplitude and frequency demodulation algorithm for a virtual dynamic AFM. *Nanotechnology*, *17*(7), S173.

[12] Sahoo, D. R., Sebastian, A., & Salapaka, M. V. (2003). Transient-signal-based sample-detection in atomic force microscopy. *Applied Physics Letters*, *83*(26), 5521-5523.

[13] Payam, A. F., Fathipour, M., & Yazdanpanah, M. J. (2009). High precision imaging for non-contact mode atomic force microscope using an adaptive nonlinear observer and output state feedback controller. *Digest Journal of Nanomaterials and Biostructures*, *4*(3), 429-442.

[14] Pishkenari, H. N., Jalili, N., & Meghdari, A. (2005, January). Acquisition of high precision images for non-contact atomic force microscopy via direct identification of sample height. In *ASME International Mechanical Engineering Congress and Exposition* (Vol. 42169, pp. 1335-1342).

[15] Sinha, A. (2005). Nonlinear dynamics of atomic force microscope with PI feedback. *Journal of Sound and Vibration*, *288*(1-2), 387-394.

[16] Balantekin, M. Ü. J. D. A. T., & Değertekin, F. L. (2011). Optimizing the driving scheme of a self-actuated atomic force microscope probe for high-speed applications. *Ultramicroscopy*, *111*(8), 1388-1394.

[17] Rana, M. S., Pota, H. R., & Petersen, I. R. (2012, December). Model predictive control of atomic force microscope for fast image scanning. In *2012 IEEE 51st IEEE Conference on Decision and Control (CDC)* (pp. 2477-2482). IEEE.

[18] Xie, S., & Ren, J. (2019). High-speed AFM imaging via iterative learning-based model predictive control. *Mechatronics*, *57*, 86-94.

[19] Fukuma, T., Kimura, M., Kobayashi, K., Matsushige, K., & Yamada, H. (2005). Development of low noise cantilever deflection sensor for multienvironment frequency-modulation atomic force microscopy. *Review of Scientific Instruments*, *76*(5).

[20] Kabaila, P. (1983). On output-error methods for system identification. *IEEE Transactions on Automatic Control*, *28*(1), 12-23.

[21] Wang, L. (2009). *Model predictive control system design and implementation using MATLAB* (Vol. 3). London: springer.